

# NMR structure of the haem core of a novel tetrahaem cytochrome isolated from *Shewanella frigidimarina*: identification of the haem-specific axial ligands and order of oxidation

Miguel Pessanha<sup>a</sup>, Lorraine Brennan<sup>a,1</sup>, António V. Xavier<sup>a</sup>, Pauline M. Cuthbertson<sup>b</sup>, Graeme A. Reid<sup>b</sup>, Stephen K. Chapman<sup>c</sup>, David L. Turner<sup>d</sup>, Carlos A. Salgueiro<sup>a,e,\*</sup>

<sup>a</sup>Instituto de Tecnologia Química e Biológica, Universidade Nova de Lisboa, Rua da Quinta Grande 6, 2780-156 Oeiras, Portugal

<sup>b</sup>Institute of Cell and Molecular Biology, University of Edinburgh, Mayfield Road, Edinburgh EH9 3JR, UK

<sup>c</sup>Department of Chemistry, University of Edinburgh, West Mains Road, Edinburgh EH9 3JJ, UK

<sup>d</sup>Department of Chemistry, University of Southampton, Southampton SO17 1BJ, UK

<sup>e</sup>Departamento de Química da Faculdade de Ciências e Tecnologia da Universidade Nova de Lisboa, Quinta da Torre, 2825-114 Caparica, Portugal

Received 14 November 2000; accepted 29 November 2000

First published online 8 January 2001

Edited by Thomas L. James

**Abstract** The tetrahaem cytochrome isolated during anaerobic growth of *Shewanella frigidimarina* NCIMB400 is a small protein (86 residues) involved in electron transfer to Fe(III), which can be used as a terminal respiratory oxidant by this bacterium. A 3D solution structure model of the reduced form of the cytochrome has been determined using NMR data in order to determine the relative orientation of the haems. The haem core architecture of *S. frigidimarina* tetrahaem cytochrome differs from that found in all small tetrahaem cytochromes *c*<sub>3</sub> so far isolated from strict anaerobes, but has some similarity to the N-terminal cytochrome domain of flavocytochrome *c*<sub>3</sub> isolated from the same bacterium. NMR signals obtained for the four haems of *S. frigidimarina* tetrahaem cytochrome at all stages of oxidation were cross-assigned to the solution structure using the complete network of chemical exchange connectivities. Thus, the order in which each haem in the structure becomes oxidised was determined. © 2001 Federation of European Biochemical Societies. Published by Elsevier Science B.V. All rights reserved.

**Key words:** Multahaem cytochrome; Nuclear magnetic resonance; Ring current; Iron-respiration; *Shewanella*

## 1. Introduction

The Gram-negative, facultatively anaerobic bacteria belonging to the genus *Shewanella* are found in a remarkable range of environments, mainly aquatic (marine, freshwater and sewage), but also in spoiling meat, fish, clinical specimens, and in natural energy reserves, where they have been implicated in

corrosion of oil pipelines [1–4]. *Shewanella* spp. can grow under anaerobic conditions as long as other electron acceptors, such as nitrogen and sulfur compounds or organic oxidants, are supplied [5]. The exceptional respiratory versatility of *Shewanella* is illustrated by its capacity to reduce Mn(III/IV) and Fe(III) oxides [5,6] as well as to dehalogenate chlorinated compounds anaerobically [7]. This confers an important role on these bacteria in the bio-geochemistry of several anaerobic environments.

The ability of *Shewanella* spp. to use such a variety of terminal electron acceptors, which span a large range of redox potentials, raises a number of interesting questions about the electron transport system, which is presently unknown. However, under anaerobic conditions these bacteria synthesise a large amount of *c*-type cytochromes that are located primarily in the outer membrane [8]. The distribution of cytochrome found in *Shewanella* spp. differs from that found in other bacteria, where cytochromes are typically confined to the periplasm and cytoplasmic membrane [9], and this may be related to a possible role played by these cytochromes in the anaerobic respiratory reduction of Fe(III) and Mn(III/IV).

Some of the cytochromes isolated from *Shewanella* spp. during anaerobic growth have been purified, characterised biochemically, and sequenced, but only a few have been subject to detailed molecular analysis. The best studied to date is flavocytochrome *c*<sub>3</sub>, which shows different physicochemical properties when compared with the well-studied phototropic bacterial flavocytochromes [10]. The X-ray structure of flavocytochromes *c*<sub>3</sub> isolated from *Shewanella frigidimarina* NCIMB400, *Sffcc*<sub>3</sub>, [11] and *Shewanella oneidensis* MR-1 [12] have been determined. The overall fold of the N-terminal cytochrome domain in these structures, which has four covalently bound haem groups with bis-histidinyl ligation, is distinct from those found in all the other haem-containing proteins.

During anaerobic growth, *Shewanella* spp. also produces a small tetrahaem *c*-type cytochrome with 86 residues. This is the smallest tetrahaem cytochrome found to date, and the first tetrahaem cytochrome isolated from a facultative anaerobe. All the other small tetrahaem cytochromes were isolated from strict anaerobic species belonging to the genus *Desulfovibrio*. Recently, it was found that the growth rate of *S. frigid-*

\*Corresponding author. Fax: (351)-21-4428766.  
E-mail: cas@itqb.unl.pt

<sup>1</sup> Present address: Department of Biochemistry, University College Dublin, Belfield, Dublin4, Ireland.

**Abbreviations:** *Sfc*, *Shewanella frigidimarina* NCIMB400 tetrahaem cytochrome; *Sffcc*<sub>3</sub>, *Shewanella frigidimarina* NCIMB400 flavocytochrome *c*<sub>3</sub>; *Dc*<sub>3</sub>s, *Desulfovibrio* spp cytochromes *c*<sub>3</sub>; *DvHc*<sub>3</sub>, *Desulfovibrio vulgaris* (Hildenborough) cytochrome *c*<sub>3</sub>; *Dgc*<sub>3</sub>, *Desulfovibrio gigas* cytochrome *c*<sub>3</sub>; NOESY, nuclear Overhauser spectroscopy; TOCSY, total correlation spectroscopy; COSY, correlation spectroscopy

*imarina* under anaerobiosis with Fe(III) as sole acceptor is severely impaired if the tetrahaem cytochrome is removed by gene disruption [13]. The primary sequence of this cytochrome isolated from *S. frigidimarina* NCIMB400, *Sfc*, has been determined [13] and comparison with cytochromes *c*<sub>3</sub> isolated from *Desulfovibrio* spp. shows that there are remarkable differences, even at the sites of haem ligation to the polypeptide chain (Fig. 1). In particular, for *Sfc* and *Sffcc*<sub>3</sub> the haem binding motif is CXXCH for all haems whereas for all the other cytochromes *c*<sub>3</sub> at least one haem shows the CXXXXCH motif [14–22]. Moreover, the conserved pattern of two consecutive haem axial ligands observed in all tetrahaem cytochromes *c*<sub>3</sub> isolated from *Desulfovibrio* spp., *Dc*<sub>3</sub>s, is not found in *Sfc*, suggesting a different haem core arrangement. However, there is no structure available for *Sfc* whereas several crystal structures of *Dc*<sub>3</sub>s were determined ([23], and references therein). Also, solution structures have been obtained from NMR data for cytochrome *c*<sub>3</sub> isolated from *Desulfovibrio vulgaris* (Hildenborough) in the reduced state [24], and for that from *Desulfovibrio gigas* in both reduced and oxidised states [15].

It is essential to obtain structural information for *Sfc* in order to interpret physicochemical data, such as thermodynamic and kinetic properties, which are essential for understanding the electron transfer properties of the protein. Therefore, we have determined the relative haem orientations, the pattern of His ligation, and the order in which the haems in the structure are oxidised in *Sfc*.

## 2. Materials and methods

The tetrahaem cytochrome isolated from *S. frigidimarina* NCIMB400 was purified as described previously [13]. For NMR experiments in H<sub>2</sub>O, the protein was lyophilised from H<sub>2</sub>O and resuspended in 92% H<sub>2</sub>O/8% <sup>2</sup>H<sub>2</sub>O to a final concentration of approximately 3 mM. For NMR experiments in <sup>2</sup>H<sub>2</sub>O, the protein was lyophilised several times with <sup>2</sup>H<sub>2</sub>O (99.96% atom). The sample was reduced by gaseous hydrogen in the presence of catalytic amounts of hydrogenase isolated from *D. vulgaris* and *D. gigas*. The pH was adjusted to 6.1 in an anaerobic chamber (Mbraun MB 150 I) by addition of 0.1 M NaO<sup>2</sup>H or <sup>2</sup>HCl, for <sup>2</sup>H<sub>2</sub>O samples, and 0.1 M NaOH or HCl, for H<sub>2</sub>O samples. The pH values determined are direct meter readings without correction for the isotope effect [25]. An antibiotic cocktail with 70 μM ampicillin, 50 μM kanamycin and 50 μM chloramphenicol was added to the sample in H<sub>2</sub>O to prevent bacterial growth.

For the NMR redox titrations, a 1 mM sample was prepared at pH 6.5 in <sup>2</sup>H<sub>2</sub>O as described above. The intermediate oxidation levels were obtained by first washing out the hydrogen from the reduced sample with argon and then adding controlled amounts of air into the NMR tube with a syringe through the serum caps.

### 2.1. NMR spectroscopy

**2.1.1. Structural studies.** <sup>1</sup>H-NMR spectra were obtained on a Bruker DRX500 spectrometer equipped with a 5 mm inverse detection probe head with internal B<sub>0</sub> gradient coils and a Eurotherm 818 temperature control unit. 2D spectra were acquired at 303 K but additional spectra were acquired at 299 K to resolve overlapping signals. All the 2D NMR spectra were acquired collecting 4096 (*t*<sub>2</sub>) × 1024 (*t*<sub>1</sub>) data points to cover a sweep width of 8 kHz, with 32 scans per increment. The <sup>2</sup>H<sub>2</sub>O nuclear Overhauser spectroscopy (NOESY) (10, 50, and 80 ms mixing time), total correlation spectroscopy (TOCSY) (40 and 80 ms mixing time) and correlation spectroscopy (COSY) spectra were acquired using standard pulse techniques. The H<sub>2</sub>O NOESY (40, 80, and 100 ms mixing time) and TOCSY (40, 60, and 80 ms mixing time) spectra were acquired using the WATERGATE sequence for water suppression [26]. The H<sub>2</sub>O COSY spectra were acquired using standard pulse techniques.

**2.1.2. Redox titrations.** 2D NOESY (25 ms mixing time) and ROESY (10 ms spin lock pulse) spectra were collected at 298 K using 4096 (*t*<sub>2</sub>) × 1024 (*t*<sub>1</sub>) data points to cover a sweep width of 38 kHz, with 128 scans per increment. In order to distinguish unequivocally all the haem methyl groups in oxidation stages 0 and 1, NOESY spectra were also acquired with a sweep width of 9 kHz.

### 2.2. Structure determination

**2.2.1. Assignment and integration.** The software package XEASY (version 1.2; ETH, Zurich, Switzerland) [27] was used to display and annotate spectra and for volume integration of NOESY cross-peaks. Amino acid assignment was performed using the classical approach described by Wüthrich [28]. Spin systems were identified through analysis of the TOCSY and COSY spectra in <sup>2</sup>H<sub>2</sub>O and H<sub>2</sub>O at different temperatures and sequence-specific assignments were obtained by identifying the sequential connectivities in the H<sub>2</sub>O NOESY spectra. All of the residues except residues 1, 2, 25, and 37, have been identified so far. Haem signals were identified by following the strategy for the assignment of haem protons in multihaem ferrocyclochromes described by Turner et al. [29]. The NOE's observed between the axial histidines and the haem protons, namely between haem meso and axial His ring protons, were used to associate the sets of haem signals with their respective CXXCH binding sites in the sequence.

**2.2.2. Structure calculations.** Assigned cross-peaks in the 80 ms H<sub>2</sub>O NOESY spectra at 303 K were integrated. The cross-peaks involving protons separated by fixed distances and all the intra-haem cross-peaks, except those involving propionate groups, were excluded and the resulting peak lists were used as input for the program INDYANA [15,30]. From these integrals, the program generated 329 lower and 324 upper limits to act as volume restraints.

In order to confirm the assignment of the haem set signals and the axial ligands, in the first stages of structure calculations, the His ligand from the CXXCH haem binding site was left free to attach to either face of the haem. This was achieved by using a fragment representing the His with pseudo-pyrrole-nitrogens attached to it [24,30] but only constraining two of them with fixed upper limit distances to the nitrogens of the haem, NA and NC. The distal histidines were left completely free. Thus the calculations allowed the sixth His ligand of each haem to be identified as well as the haem faces to which each ligand is attached. In subsequent calculations, the axial ligands were constrained to the positions that had been identified, in order to improve convergence.

## 3. Results and discussion

### 3.1. Haem core architecture

The NMR spectra of the tetrahaem ferrocyclochrom isolated from *S. frigidimarina* NCIMB400 (*Sfc*) shows eight sharp signals from His rings with chemical shifts typical of haem axial ligands (data not shown). The NOE's observed between the haem meso protons and the axial His were used to obtain the specific assignment of the four haems confirming that the four haems have bis-histidinyl axial coordination, which correlates with the low redox potentials observed for the cytochrome and is supported by the EPR spectrum [13]. The structure model obtained accordingly to the methodology described in Section 2 (Fig. 2A), confirmed the haem specific assignments, as well as those of the axial ligands, and allows the identification of the haem faces to which they are attached. Numbered according to the order of attachment to the polypeptide chain, haem I is axially coordinated by His 19 and His 65; haem II by His 9 and His 39; haem III by His 49 and His 62; and finally haem IV by His 52 and 79, with the distal (sixth) ligand in bold. The relative position of the haem axial ligands in the primary sequence of *Sfc* and that found in the N-terminal cytochrome domain of *Sffcc*<sub>3</sub> [11] is the same (Fig. 1A). The haem faces to which each ligand is attached are also the same in both cytochromes.

The *Sfc* haem spatial arrangement is responsible for the

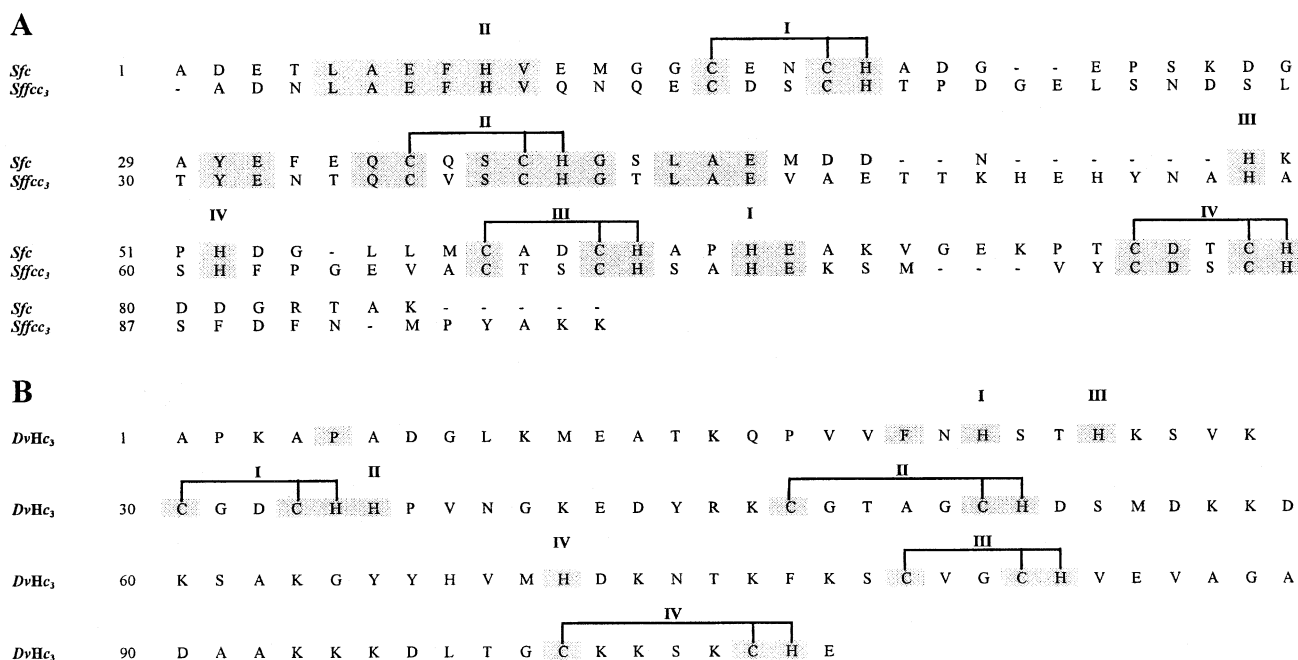


Fig. 1. Comparison between the relative positions of the haem binding motifs and haem axial ligands in both the tetrahaem and the N-terminal cytochrome domain of flavocytochrome  $c_3$  isolated from *S. frigidimarina* and the *Desulfovibrio* spp. cytochromes  $c_3$ . A: Alignment of the polypeptide sequences of *Sfc* and *Sffcc<sub>3</sub>* N-terminal cytochrome domain. The grey shadowed letters indicate the conserved residues in these two proteins. B: Primary sequence of *D. vulgaris* (Hildenborough) cytochrome  $c_3$ , *DvHc<sub>3</sub>* [14]. This sequence was chosen to represent all cytochromes  $c_3$  isolated from *Desulfovibrio* species: *D. gigas* [15], *D. desulfuricans* (El Agheila Z) [16], *Desulfovibrio salexigens* [17], *Desulfovibrio norvegicum* [18], *D. vulgaris* (Miyazaki F) [19], *D. desulfuricans* (ATCC 27774) [20] and acidic and basic proteins from *Desulfovibrio africanus* [21]. The grey shadowed letters indicate the residues conserved in all *Dc<sub>3</sub>s*. The bold roman numbers in (A) and (B) indicate the haem binding motifs (CXX(XX)CH) and the sixth axial ligand of each haem.

large and unusual chemical shift span observed for some haem substituents in the reduced form (Table 1). The meso protons  $20\text{H}^{\text{II}}$  and  $20\text{H}^{\text{III}}$ , as well as the haem methyls  $18^{\text{I}}\text{CH}_3^{\text{II}}$ ,  $2^{\text{I}}\text{CH}_3^{\text{III}}$ ,  $18^{\text{I}}\text{CH}_3^{\text{III}}$  and haem thioether methyl  $8^{\text{I}}\text{CH}_3^{\text{III}}$  are shifted far upfield due to the contribution of the ring current shifts of neighbouring aromatic rings (Fig. 3). The accuracy of the haem proton assignment (Table 1) and the NMR solution structure model of *Sfc* were tested simultaneously by comparing the calculated and observed haem proton chemical shifts (Fig. 3). These shifts correlate very well even for the protons subject to the larger ring current effects.

Comparison between the structures of *Sfc* and tetrahaem cytochromes  $c_3$  isolated from *Desulfovibrio* spp., *Dc<sub>3</sub>s* (Fig. 2) shows that, as expected from the differences observed in the

primary sequence, there are important modifications both at the level of the haem core architecture and at the level of the general folding. In fact, the cross-links resulting from the location of haem axial ligands in the polypeptide chain, the lack of the two consecutive axial histidines, and the haem binding motifs explain the enormous difference observed in the spatial disposition of the haems in the two types of tetrahaem cytochromes (Fig. 2): (i) in *Dc<sub>3</sub>s* the distal axial ligands are located in the sequence in the following order: I, III, II and IV whereas in *Sfc* they appear in the primary sequence in the order II, III, IV and I; (ii) the positions of the distal axial ligands in relation to the haem binding motifs are also quite different in both types of proteins (Fig. 1). In *Dc<sub>3</sub>s* the distal axial ligands of haems I and III are located before the binding site of haem I, the distal ligand of haem II is found between the binding sites of haem I and II, and the distal ligand of haem IV is located between the binding sites of haem II and III. By contrast, in *Sfc*, the distal axial ligand of haem II is located before the binding site of haem I, there are no distal ligands located between haem I and II, and the two distal ligands of haem III and IV are located between haem binding motifs II and III. Finally, the distal ligand of haem I is located between the binding motifs of haems III and IV.

Interestingly, the haem core architecture is strictly maintained in *Dc<sub>3</sub>s* despite the low homologies between their amino acid sequences. Apart from the residues involved in the haem ligation, only two other residues are conserved (Fig. 1B). The conserved pattern of consecutive axial ligands for haem I (fifth ligand) and haem II (sixth ligand) in the sequence is an important constraint that is largely responsible for the haem core architecture adopted by these cytochromes.

Table 1  
Chemical shifts (ppm) of the haem substituents in *S. frigidimarina* NCIMB400 tetrahaem ferrocyclochrome, at pH 6.1 and 303 K

Haem substituent	I	II	III	IV
5H	8.99	9.45	9.08	9.78
10H	8.72	9.39	8.62	9.55
15H	9.67	9.73	9.72	9.42
20H	9.29	7.73	7.33	9.51
$2^{\text{I}}\text{CH}_3$	3.59	2.66	1.81	3.61
$7^{\text{I}}\text{CH}_3$	3.13	3.67	2.80	3.98
$12^{\text{I}}\text{CH}_3$	3.40	3.45	3.46	3.55
$18^{\text{I}}\text{CH}_3$	3.18	1.14	1.83	3.26
$3^{\text{I}}\text{H}$	5.69	6.53	5.79	5.98
$8^{\text{I}}\text{H}$	5.76	6.34	5.20	6.46
$3^{\text{I}}\text{CH}_3$	2.10	2.69	1.85	2.62
$8^{\text{I}}\text{CH}_3$	-0.05	2.48	-1.03	2.47

The haems are numbered according to the IUPAC-IUB nomenclature for tetrapyrroles [45].

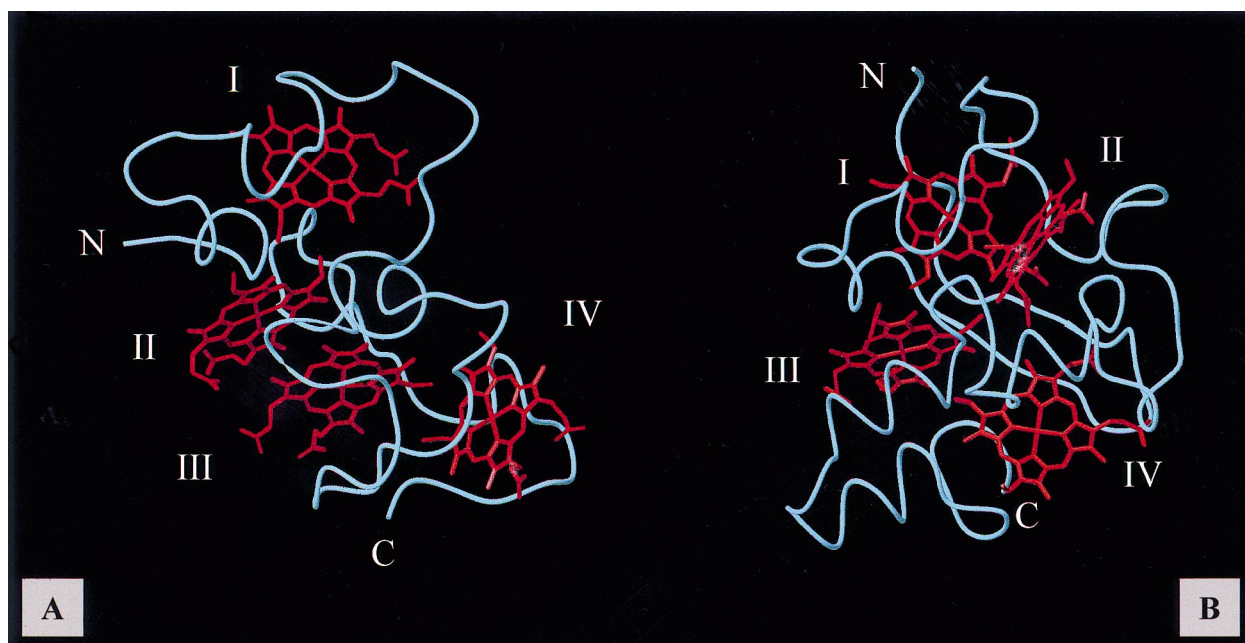


Fig. 2. Haem core solution structures of the *S. frigidimarina* tetrahaem ferrocytochrome (A) and *D. vulgaris* (Hildenborough) ferrocytochrome  $c_3$  [24] (B). The haems and the  $\alpha$ -carbon chain in *Sfc* correspond to the structure with the lowest target function out of 200 structures annealed from random starting points (see legend of Table 2). The haem groups are indicated by roman numbers. The N- and C-terminus of the polypeptide chains are indicated by the letters N and C, respectively. The structures were oriented so that haem I can be superimposed in both ferrocytochromes.

Haems I and IV are approximately parallel, but perpendicular to haems II and III, which are perpendicular to each other. The overall fold of the polypeptide chain is conserved as a result of the similar organisation of the haem binding resi-

dues. The structure forms two domains, one of which contains haem I and the other binds haem IV. Haem III is located in a groove that defines part of the interdomain region and is attached to residues located in both domains, with its binding residues interlaced with those of haem I and IV in the polypeptide chain. Haem II is also located in the interdomain region but the residues which bind it do not have residues binding other haems between them [18]. Furthermore, the architecture of the *Desulfofuromonas acetoxidans* tri-haem cyto-

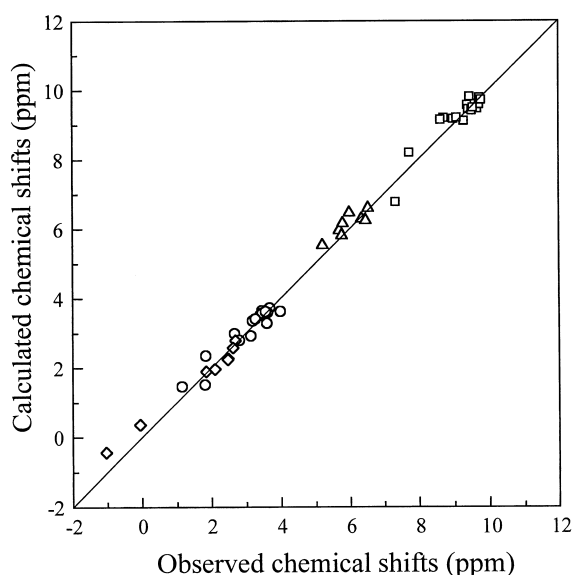


Fig. 3. Comparison between the calculated and observed chemical shifts for the haem substituents of reduced *Sfc*. The haem substituent chemical shifts were calculated by correcting the haem protons reference shifts (9.36 ppm for haem meso protons, 6.13 for haem thioether methines, 3.48 for haem methyls, and 2.12 for haem thioether methyls [44]) with the ring current shifts calculated from the best *Sfc* NMR reduced structure accordingly to the procedure described by Messias et al. and Turner et al. [24,29]. The meso protons, thioether methines, methyls, and thioether methyls are represented by squares, triangles, circles and diamond symbols, respectively. The straight line has a unit slope.

Table 2  
Haem core characteristics of tetrahaem cytochromes isolated from *S. frigidimarina* NCIMB400 and from the *Desulfovibrio* genus

	Haem	I	II	III	IV
<i>Sfc</i>	I		6.3 (0.2)	11.0 (0.4)	16.6 (0.9)
<i>Sffcc</i> <sub>3</sub>			6.2	12.2	22.0
<i>Dgc</i> <sub>3</sub>			6.4	6.0	10.7
<i>Sfc</i>	II	12.2 (0.2)		3.3 (0.1)	15.3 (0.2)
<i>Sffcc</i> <sub>3</sub>		12.5		3.9	17.6
<i>Dgc</i> <sub>3</sub>		12.0		8.3	10.8
<i>Sfc</i>	III	15.9 (0.3)	9.2 (0.1)		6.0 (0.2)
<i>Sffcc</i> <sub>3</sub>		17.3	9.5		8.0
<i>Dgc</i> <sub>3</sub>		11.2	15.5		5.5
<i>Sfc</i>	IV	23.1 (0.7)	20.1 (0.4)	11.5 (0.3)	
<i>Sffcc</i> <sub>3</sub>		29.8	25.0	15.6	
<i>Dgc</i> <sub>3</sub>		18.0	16.7	12.0	

Comparison with the haem core of the N-terminal cytochrome domain of flavocytochrome  $c_3$  isolated from *S. frigidimarina* NCIMB400 [11] is also indicated. The conserved haem core of cytochrome  $c_3$  isolated from *Desulfovibrio* is illustrated by *D. gigas* cytochrome  $c_3$ , *Dgc*<sub>3</sub> [33]. The intramolecular iron-to-iron distances (Å) are given below the centre diagonal and porphyrin edge-to-edge distances (Å) are given above it. The values for *Sfc* correspond to the average of the 20 best structures from 200 random starting structures annealed, which cover a 10% range of target functions (with standard deviations in parentheses).

Table 3

Redox-dependent haem methyl chemical shifts in the tetrahaem cytochrome from *S. frigidimarina*, at pH 6.5 and 298 K

Oxidation stage	Chemical shift (ppm)				$x_i$				$\Sigma x_i$
	I	II	III	IV	I	II	III	IV	
0	3.24	3.52	1.89	3.32	0	0	0	0	0
1	6.90	9.20	7.93	17.31	0.105	0.264	0.164	0.462	0.995
2	15.50	17.09	10.28	28.44	0.353	0.631	0.227	0.830	2.041
3	34.93	21.20	15.17	32.16	0.912	0.822	0.360	0.952	3.046
4	37.99	25.02	38.83	33.60	1	1	1	1	4

The haem methyls  $18^1\text{CH}_3^{\text{I}}$ ,  $12^1\text{CH}_3^{\text{II}}$ ,  $2^1\text{CH}_3^{\text{III}}$  and  $18^1\text{CH}_3^{\text{IV}}$  were chosen to monitor each haem oxidation through the five oxidation stages. The haem oxidation fractions,  $x_i$ , are obtained from the paramagnetic shifts.

chrome  $c_{551.5}$  is essentially similar to that of these cytochromes  $c_3$ , but with haem II deleted [31,32].

In contrast, the overall fold of the tetrahaem cytochrome isolated from *Sf* has no relation with those from the genus *Desulfovibrio* (cf. [33]) and is more similar to the ‘dog-leg’ arrangement observed in the N-terminal cytochrome domain of *Sffcc*<sub>3</sub> (cf. [11]). This is probably due to the fact that all the haem binding residues of *Sfc* and *Sffcc*<sub>3</sub> are similarly interlaced in the polypeptide chain but in a rather different order from that found in *Dc*<sub>3</sub>s (Fig. 1). Like in *Dc*<sub>3</sub>s, the polypeptide chain in *Sfc* also forms two distinct domains (1–41 and 42–86), but here only haem I shares ligands from residues of two domains. As in *Sffcc*<sub>3</sub>, haems I and II are approximately perpendicular, haem II is roughly parallel to haem III, and haem IV is approximately perpendicular to haem III, but haem IV is closer to the other haem groups (Table 2). The relative location of the axial ligands and the haem binding motifs is the same in *Sfc* and the *Sffcc*<sub>3</sub>, but a difference in the spatial position of haem IV between *Sfc* and *Sffcc*<sub>3</sub> is not unexpected since in the tetrahaem cytochrome this haem is not stabilised by the dimethylbenzene portion of the FAD isoalloxazine ring of the flavocytochrome [11]. The different orientation of haem IV observed in *Sfc* may be required for the thermodynamic stabilisation and to maximise haem–haem interactions that facilitate electron transfer between haems since much smaller edge-to-edge and iron-to-iron distances are observed (Table 2).

The more linear arrangement of the haems in *Sfc* is reminiscent of that observed in the much larger tetrahaem cytochrome subunit of the *Rhodopseudomonas viridis* reaction centre (cf. [34]). However, in *Sfc* the spatial haem disposition is not quite as linear.

### 3.2. Order of oxidation of the haem groups

The *Sfc* is much more similar to other proteins from *Shewanella* spp. [13], such as the N-terminal cytochrome domain of *Sffcc*<sub>3</sub> [35,36], than it is to *Dc*<sub>3</sub>s. In terms of the primary sequence, the two *Sf* cytochromes show very little sequence similarity with *Dc*<sub>3</sub>s (average identity of 12%) and yet they share important properties. All of the haem irons have bis-His axial coordination and they are low spin, both in the reduced and oxidised forms. Thus, the protein is diamagnetic when reduced (Fe(II),  $S=0$ ) and paramagnetic when oxidised (Fe(III),  $S=1/2$ ). This is convenient for NMR studies since widely different well-resolved spectra are obtained for both oxidation states, making it easier to assign the order in which specific haems within the structure are oxidised. The NMR spectrum of a partially oxidised sample at pH 6.5 shows that the cytochrome exhibits fast intramolecular and slow intermolecular electron exchange on the NMR time scale (data not

shown). In these conditions, signals from the 16 redox microstates are averaged in five groups of oxidation stages, each including the microstates with the same number of oxidised haems [37]. Therefore, the substituents of each haem have different chemical shifts in the five macroscopic oxidation stages and, since these paramagnetic shifts are proportional to the degree of oxidation of that particular haem group, they can be used to monitor the oxidation of each haem throughout the redox titration. Thus, signals from individual haem substituents, namely haem methyls, were followed through the NMR spectra of a redox titration from the fully reduced to the fully oxidised form (Table 3).

The influence of the oxidation of neighbouring haems on the paramagnetic shift of a haem methyl group of a different haem (extrinsic shift) can not be determined accurately at this stage. Therefore, haem methyl groups pointing out towards the protein surface were chosen for determining the order of haem oxidation according to the procedure described by Salgueiro et al. [38]. The paramagnetic chemical shifts of haem methyl groups  $18^1\text{CH}_3^{\text{I}}$ ,  $12^1\text{CH}_3^{\text{II}}$ ,  $2^1\text{CH}_3^{\text{III}}$  and  $18^1\text{CH}_3^{\text{IV}}$  at pH 6.5 were used to calculate the oxidation fraction of each haem at different stages of oxidation (Table 3). Analysis of Table 3 confirms that the extrinsic shifts for the haem methyl groups chosen are not significant since the sums of the oxidation fraction at each oxidation stage are very close to integers. Analysis of this table also gives the order of oxidation of the haems, which is very different from those observed in *Dc*<sub>3</sub>s studied so far [38–41]: haem IV is the haem that becomes more oxidised by the first redox step (stage 1), the largest fractional oxidation of haem II is obtained by the second step (stage 2), which is followed by haem I (stage 3) and finally by haem III (stage 4).

Finally, it is worth noting that *S. frigidimarina* tetrahaem cytochrome can be reduced by *Desulfovibrio* hydrogenases. This indicates that the *Shewanella* hydrogenase may have a similar coupling function with its tetrahaem cytochromes [42]. In fact, analysis of the genome of *S. oneidensis* MR-1 [43] reveals that this bacterium contains a hydrogenase, which shares about 50% identity with *D. vulgaris* and *D. gigas* [Ni–Fe] hydrogenases.

**Acknowledgements:** We would like to acknowledge to Dr António Maretzek for technical support with NMR and software. This work was supported by EC Contract FMRX-CT98-0218.

### References

- [1] Semple, K.M., Doran, J.L. and Westlake, D.W.S. (1989) Can. J. Microbiol. 35, 925–931.
- [2] Gram, L. and Huss, H.H. (1996) Int. J. Food Microbiol. 33, 121–137.

- [3] Dhawan, B., Chaudhry, R., Mishra, B.M. and Agarwal, R. (1998) *J. Clin. Microbiol.* 36, 2394.
- [4] Reid, G.A. and Gordon, E.H.J. (1999) *Int. J. Syst. Bacteriol.* 49, 189–191.
- [5] Myers, C.R. and Nealsen, K.H. (1988) *Science* 240, 1319–1321.
- [6] Myers, C.R. and Nealsen, K.H. (1990) *J. Bacteriol.* 172, 6232–6238.
- [7] Picardal, F.W., Arnold, R.G., Couch, H., Little, A.M. and Smith, M.E. (1993) *Appl. Environ. Microbiol.* 59, 3763–3770.
- [8] Myers, C.R. and Myers, J.M. (1992) *J. Bacteriol.* 174, 3429–3438.
- [9] Thöny-Meyer, L., Ritz, D. and Hennecke, H. (1994) *Mol. Microbiol.* 12, 1–9.
- [10] Gordon, E.H.J., Pealing, S.L., Chapman, S.K., Ward, F.B. and Reid, G.A. (1998) *Microbiology* 144, 937–945.
- [11] Taylor, P., Pealing, S.L., Reid, G.A., Chapman, S.K. and Walkinshaw, M.D. (1999) *Nature Struct. Biol.* 6, 1108–1112.
- [12] Leys, D., Tsapin, A.S., Nealsen, K.H., Meyer, T.E., Cusanovich, M.A. and Beeumen, J.J.V. (1999) *Nature Struct. Biol.* 6, 1113–1117.
- [13] Gordon, E.H.J., Pike, A.D., Hill, A.E., Cuthbertson, P.M., Chapman, S.K. and Reid, G.A. (2000) *Biochem. J.* 349, 153–158.
- [14] Ambler, R.P. (1968) *Biochem. J.* 109, 47–48.
- [15] Brennan, L., Turner, D.L., Messias, A.C., Teodoro, M.L., LeGall, J., Santos, H. and Xavier, A.V. (2000) *J. Mol. Biol.* 298, 61–82.
- [16] Ambler, R.P., Bruschi, M. and LeGall, J. (1971) *FEBS Lett.* 18, 347–350.
- [17] Ambler, R.P. (1973) *Syst. Zool.* 22, 554–565.
- [18] Haser, R., Pierrot, M., Frey, M., Payan, F., Astier, J.P., Bruschi, M. and LeGall, J. (1979) *Nature Lond.* 282, 806–810.
- [19] Shinkai, W., Hase, T., Yagi, T. and Matsubara, H. (1980) *J. Biochem. Tokyo* 87, 1747–1756.
- [20] Simões, P., Matias, P.M., Morais, J., Wilson, K., Dauter, Z. and Carrondo, M.A. (1998) *Inorg. Chim. Acta* 273, 213–224.
- [21] Magro, V., Pieulle, L., Forget, N., Guigliarelli, B., Petillot, Y. and Hatchikian, E.C. (1997) *Biochim. Biophys. Acta* 1342, 149–163.
- [22] Salgueiro, C.A. (1998) Caracterização estrutural e termodinâmica do citocromo  $c_3$  de *D. vulgaris*, Ph.D. Thesis, Universidade Nova Lisboa, Lisbon.
- [23] Norager, S., Legrand, P., Pieulle, L., Hatchikian, C. and Roth, M. (1999) *J. Mol. Biol.* 290, 881–902.
- [24] Messias, A.C., Kastrau, D.H.W., Costa, H.S., LeGall, J., Turner, D.L., Santos, H. and Xavier, A.V. (1998) *J. Mol. Biol.* 281, 719–739.
- [25] Glasoe, P.K. and Long, F.A. (1960) *J. Phys. Chem.* 64, 188–191.
- [26] Piotto, M., Saudek, V. and Slenar, V. (1992) *J. Biomol. NMR* 2, 661–665.
- [27] Bartels, C., Xia, T., Billeter, M., Güntert, P. and Wüthrich, K. (1995) *J. Biomol. NMR* 6, 1–10.
- [28] Wüthrich, K. (1986) *NMR of Proteins and Nucleic Acids*, John Wiley and Sons, New York.
- [29] Turner, D.L., Salgueiro, C.A., LeGall, J. and Xavier, A.V. (1992) *Eur. J. Biochem.* 210, 931–936.
- [30] Turner, D.L., Brennan, L., Meyer, H.E., Lohaus, C., Siethoff, C., Costa, H.S., Gonzalez, B., Santos, H. and Suárez, J.E. (1999) *Eur. J. Biochem.* 264, 833–839.
- [31] Coutinho, I.B., Turner, D.L., Ming, Y.L., LeGall, J. and Xavier, A.V. (1996) *J. Biol. Inorg. Chem.* 1, 305–311.
- [32] Assfalg, M., Banci, L., Bertini, I., Bruschi, M. and Turano, P. (1998) *Eur. J. Biochem.* 256, 261–270.
- [33] Matias, P.M., Morais, J., Coelho, R., Carrondo, M.A., Wilson, K., Dauter, Z. and Sieker, L. (1996) *Protein Sci.* 5, 1342–1354.
- [34] Deisenhofer, J., Epp, O., Sinning, I. and Michel, H. (1995) *J. Mol. Biol.* 246, 429–457.
- [35] Morris, C.J., Gibson, D.M. and Ward, F.B. (1990) *FEMS Microbiol. Lett.* 69, 259–262.
- [36] Dobbin, P.S., Butt, J.N., Powell, A.K., Reid, G.A. and Richardson, D.J. (1999) *Biochem. J.* 342, 439–448.
- [37] Santos, H., Moura, J.J.G., Moura, I., LeGall, J. and Xavier, A.V. (1984) *Eur. J. Biochem.* 141, 283–296.
- [38] Salgueiro, C.A., Turner, D.L., Santos, H., LeGall, J. and Xavier, A.V. (1992) *FEBS Lett.* 314, 155–158.
- [39] Louro, R.O., Pacheco, I., Turner, D.L., LeGall, J. and Xavier, A.V. (1996) *FEBS Lett.* 390, 59–62.
- [40] Salgueiro, C.A., Turner, D.L., LeGall, J. and Xavier, A.V. (1997) *J. Biol. Inorg. Chem.* 2, 343–349.
- [41] Louro, R.O., Catarino, T., Turner, D.L., Piçarra-Pereira, M.A., Pacheco, I., LeGall, J. and Xavier, A.V. (1998) *Biochemistry* 37, 15808–15815.
- [42] Louro, R.O., Catarino, T., LeGall, J. and Xavier, A.V. (1997) *J. Biol. Inorg. Chem.* 2, 488–491.
- [43] Preliminary sequence data were obtained from The Institute for Genomic Research website at <http://www.tigr.org>.
- [44] Piçarra-Pereira, M.A., Turner, D.L., LeGall, J. and Xavier, A.V. (1993) *Biochem. J.* 294, 909–915.
- [45] IUPAC-IUB Joint Comission on Biochemical Nomenclature (JCBN), (1988) *Eur. J. Biochem.* 178, 277–328.